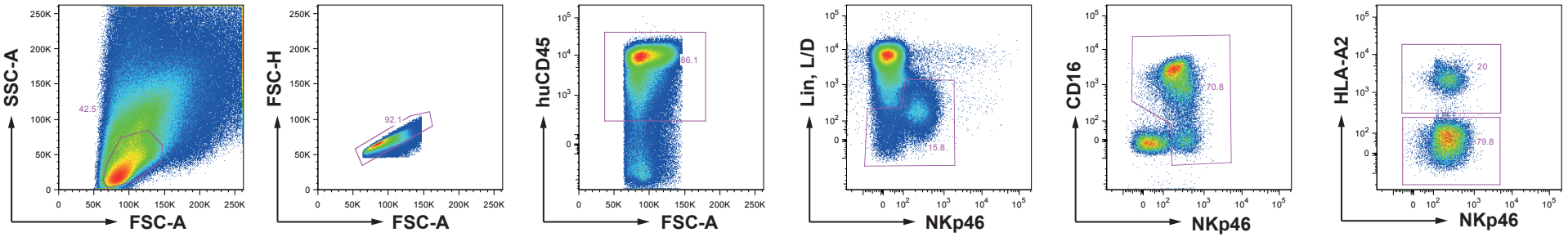

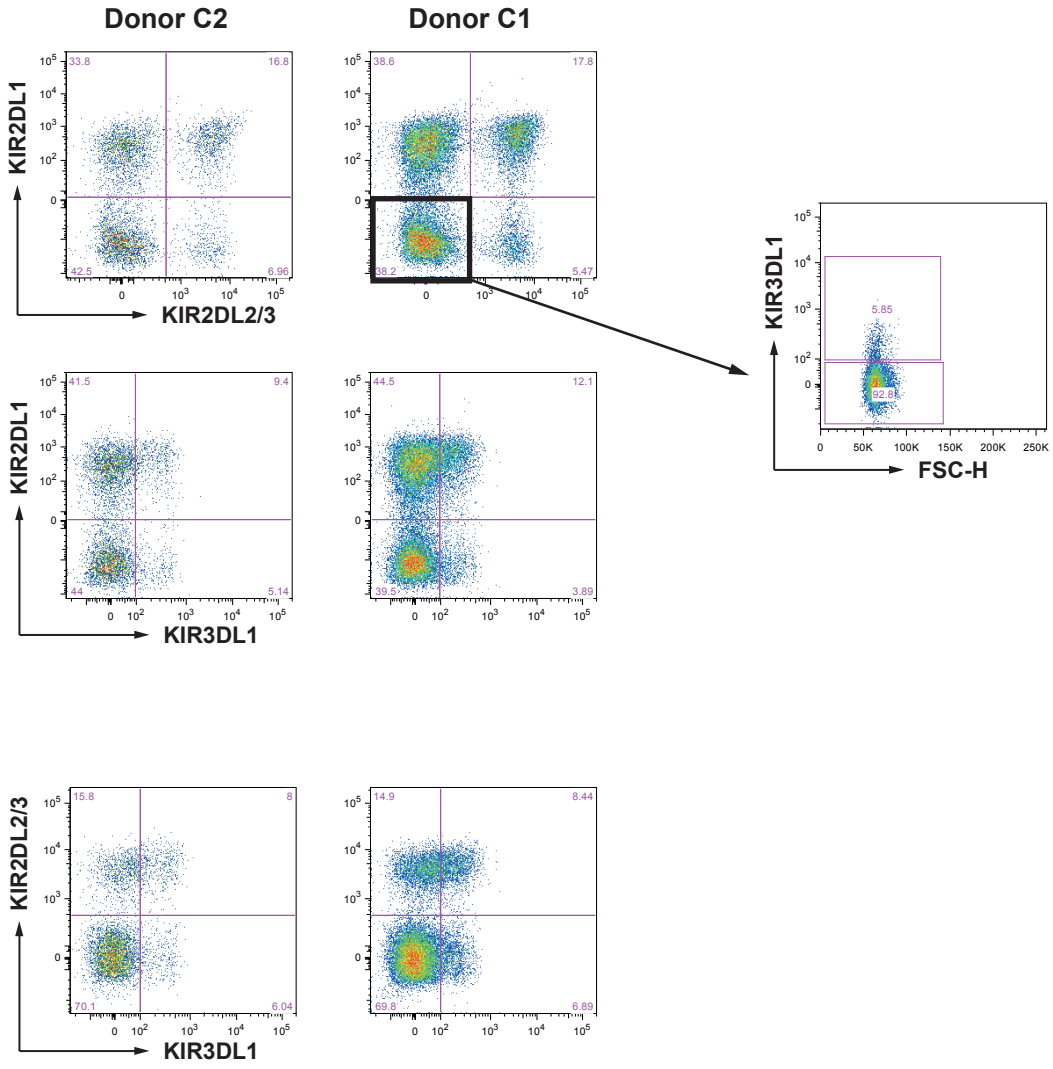

Figure S1, related to Figure 2. Gating strategy of KIR subsets.

Spleen and livers of huNSG were processed and stained with fluorescent markers for flow cytometry. Cells were pre-gated on lymphocytes and singlets before discriminating for the huCD45$^+$ population. HuCD45$^+$ lymphocytes were gated on Lin$^-$, L/D$^-$ vs. NKp46. NKp46$^+$ cells were further characterized by CD16 to arrive at the NK cell population. NK cells were assessed according to HLA-A2 for their donor origin and then gated on KIR expression. To arrive at single positive KIR populations, double negative quadrants were gated on the third parameter as shown in a representative plot. Gatings for KIR subsets were replicated in all the necessary combinations.

Figure S1
related to Figure 2

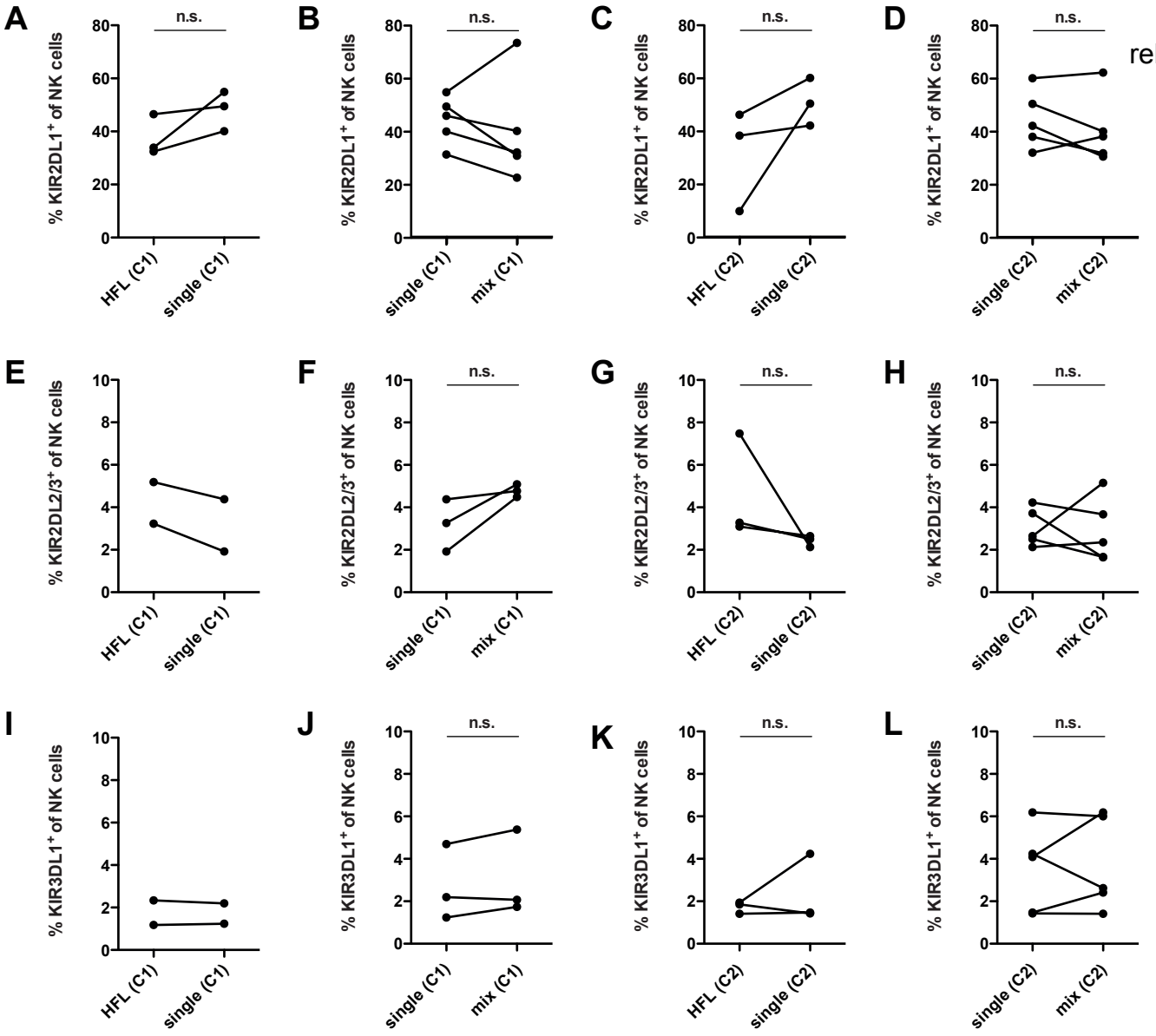

Figure S2
related to Figure 2

Figure S2, related to Figure 2. KIR frequencies at steady state represent original donor values and do not change in presence of non-cognate HLA in trans.

HuNSG mice were single reconstituted with donors homozygous for HLA-C and -B allotypes (HLA-C1, -C2 and -Bw4) or reconstituted with two donors disparate for allotype and HLA-A2 expression (mix).

(A to L) Mean percentage per experiment of single KIR$^+$ liver NK cells as derived from total NK cells of huNSG mice.

(A to D) KIR2DL1$^+$ NK cells of HLA-C1 single reconstituted huNSG mice as compared to HLA-C1 donor HFL NK cells (A) or HLA-C1 donor derived cells from mixed reconstituted huNSG mice (B) and conversely for HLA-C2 single reconstituted huNSG mice to HLA-C2 donor HFL (C) or HLA-C2 donor derived cells from mixed reconstituted huNSG mice (D).

(E to H) KIR2DL2/3$^+$ NK cells of HLA-C1 single reconstituted huNSG mice as compared to HLA-C1 donor HFL NK cells (E) or HLA-C1 donor derived cells from mixed reconstituted huNSG mice (F) and conversely for HLA-C2 single reconstituted huNSG mice to HLA-C2 donor HFL (G) or HLA-C2 donor derived cells from mixed reconstituted huNSG mice (H).

(I to L) KIR3DL1$^+$ NK cells of HLA-C1 single reconstituted huNSG mice as compared to HLA-C1 donor HFL NK cells (I) or HLA-C1 donor derived cells from mixed reconstituted huNSG mice (J) and conversely for HLA-C2 single reconstituted huNSG mice to HLA-C2 donor HFL (K) or HLA-C2 donor derived cells from mixed reconstituted huNSG mice (L).

Data are pooled data from at least three independent experiments. Dots represent mean of population in separate experiments, paired t test, n.s., not significant.

Figure S3
related to Figure 3

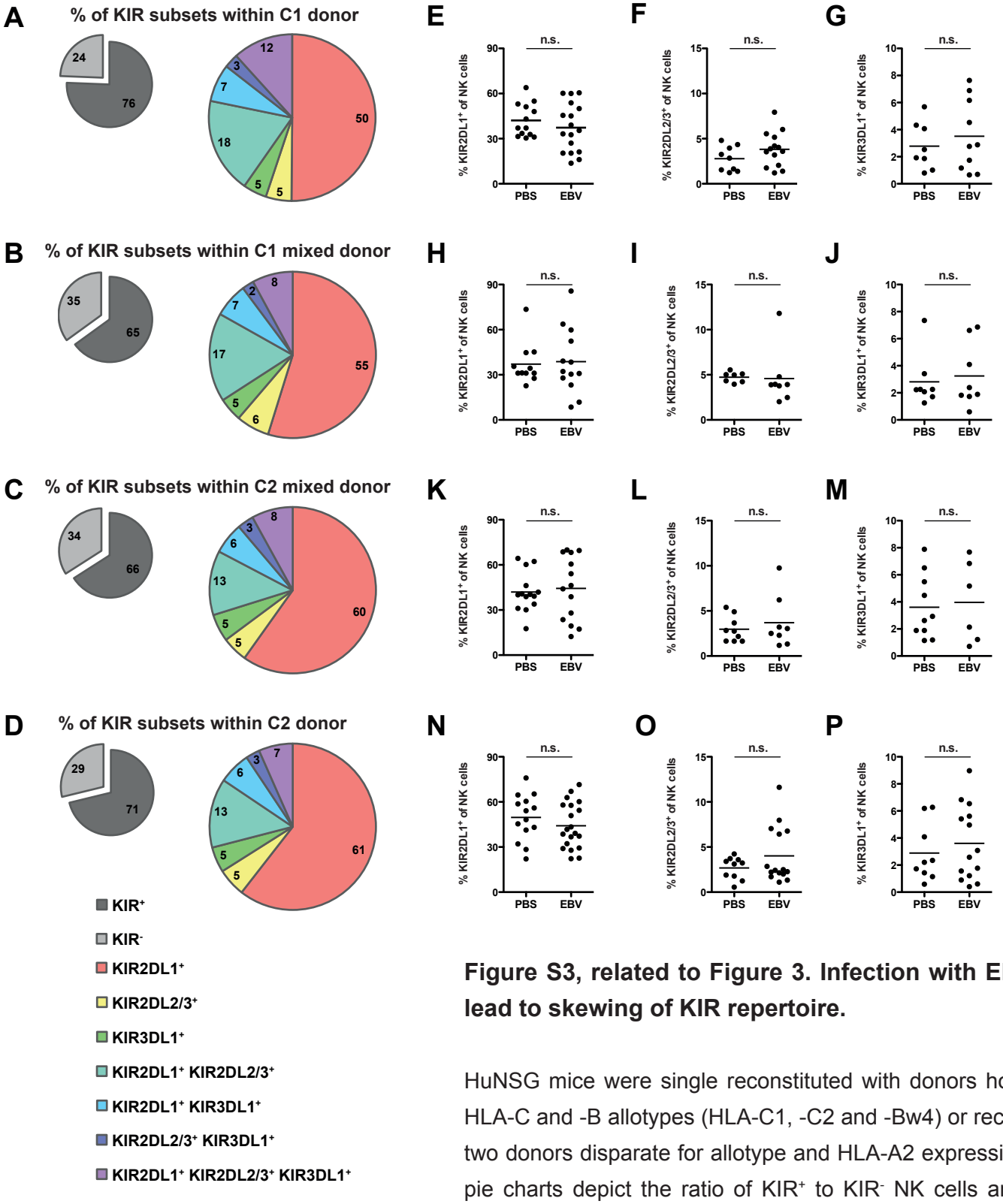

Figure S3, related to Figure 3. Infection with EBV does not lead to skewing of KIR repertoire.

HuNSG mice were single reconstituted with donors homozygous for HLA-C and -B allotypes (HLA-C1, -C2 and -Bw4) or reconstituted with two donors disparate for allotype and HLA-A2 expression (mix). Grey pie charts depict the ratio of KIR$^+$ to KIR$^-$ NK cells and colored pie charts represent the indicated KIR$^+$ NK cell subsets.

(A to D) Subsets of KIR expressing NK cells as percentages of total KIR$^+$ NK cells in liver of EBV infected huNSG mice.

(E to P) Frequency of single KIR$^+$ NK cells in liver of huNSG at endpoint. Comparison of PBS controls to EBV infected animals for frequency of KIR2DL1$^+$, KIR2DL2/3$^+$ or KIR3DL1$^+$ NK cells in homozygously reconstituted huNSG mice with HLA-C1 donor (E to G), mixed donor reconstituted huNSG mice with cells derived from HLA-C1 donor (H to J) or HLA-C2 donor (K to M) and homozygously reconstituted huNSG mice with HLA-C2 donor (M to P).

Data are pooled data from at least three independent experiments. n=8-15 mice per group, bar represents mean in relevant graphs, unpaired t test, n.s., not significant.

Figure S4
related to Figure 4

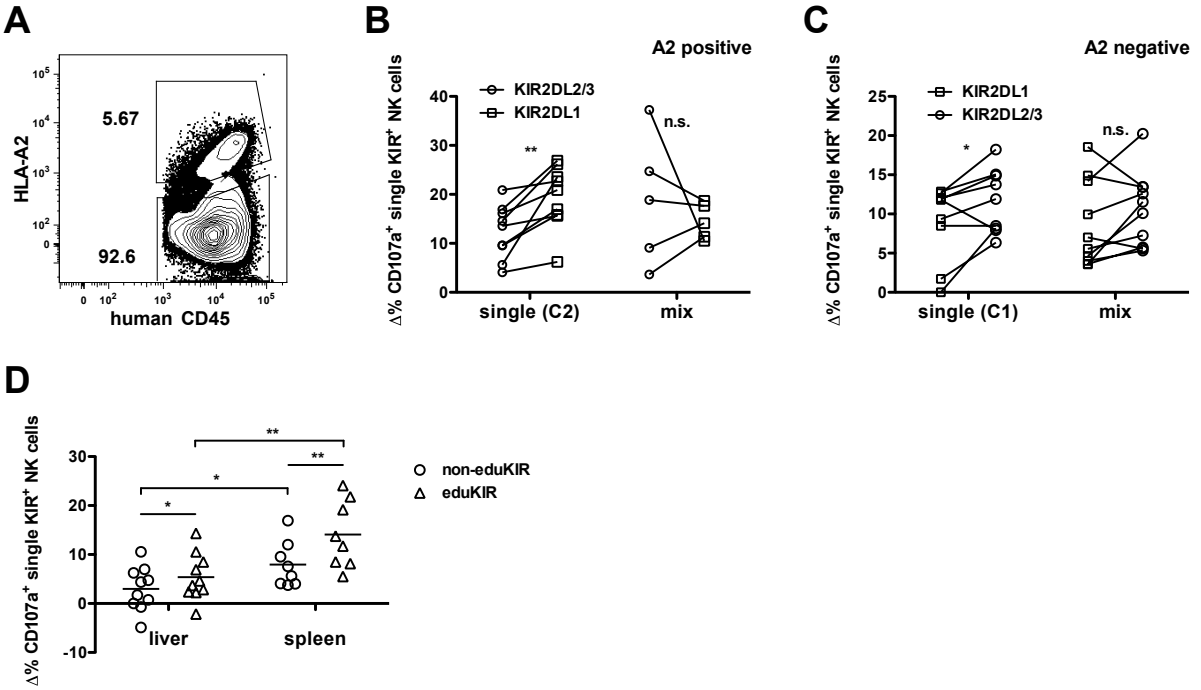

Figure S4, related to Figure 4. No titrating effect of non-cognate MHC class I on human NK cell education and decreased degranulation with lower education in liver NK cells.

HuNSG mice were single reconstituted with donors homozygous for HLA-C and -B allotype (HLA-C1 or C2) or reconstituted with both the same HLA-C1 and C2 donor disparate for HLA-A2.

(A) Representative dot plot showing overall human leukocyte reconstitution derived from HLA-C1 donor (A2 negative) and C2 donor (A2 positive) in double reconstituted huNSG mice (mix) with unequal reconstitution discovered by chance in subsets of mice. Average ± s.e.m. of C2 donor reconstitution (% frequency of HLA-A2+ in human CD45+ leukocytes) in these mice was 4.07 ± 1.27 (n=10).

(B and C) Degranulation of single KIR$^+$ NK cells after incubation of K562 cells with splenocytes from huNSG mice reconstituted with HLA-C1 homozygous and/or HLA-C2 homozygous donors from the same experiment as shown in (A). Single KIR$^+$ NK cells were gated in both single and mixed reconstituted huNSG mice on cells derived from (B) HLA-C2 A2 positive donor or from (C) HLA-C1 A2 negative donor (n=5-10 mice per group). Δ%CD107a refers to the difference of degranulation with and without K562 re-stimulation. Average ± s.e.m. of spontaneous degranulation was 1.94 % ± 0.50.

(D) Comparison of degranulation of single KIR$^\pm$ non-educated (non-eduKIR) versus educated (eduKIR) NK cells derived from liver or spleen of single donor reconstituted huNSG mice after co-culture with K562 cells (n=8-10 mice per group). Δ%CD107a refers to the difference of degranulation with and without K562 re-stimulation. Average ± s.e.m. of spontaneous degranulation was 2.30 % ± 0.68.

Data in (A) to (C) are pooled data from two independent experiments, data in (D) show data from one representative experiment. Data were analyzed by multiple t tests, *$p < 0.05$, p**< 0.01.

Figure S5
related to Figure 6

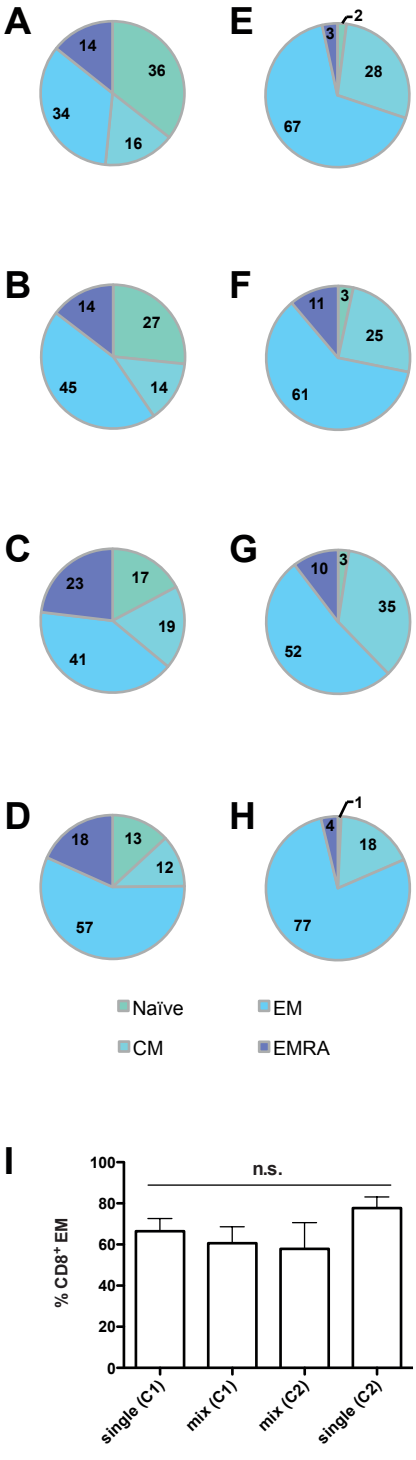

Figure S5, related to Figure 6. No change in T cell response of different reconstitutions.

HuNSG mice were single reconstituted with donors homozygous for HLA-C and -B allotypes (HLA-C1, -C2 and -Bw4) or reconstituted with two donors disparate for allotype and HLA-A2 expression (mix).

(A to I) Frequencies in percent of T cell subsets in spleens of huNSG mice at experimental endpoints.

(A to D) $CD8^+$ T cell subsets in PBS control huNSG mice single reconstituted with homozygous HLA-C1 donor (A), HLA-C2 donor (D) or mixed donor reconstituted huNSG mice with T cells derived from HLA-C1 donor (B) and derived from HLA-C2 donor (C).

(E to H) $CD8^+$ T cell subsets in EBV infected huNSG mice single reconstituted with homozygous HLA-C1 donor (E), HLA-C2 donor (H) or mixed donor reconstituted huNSG mice with T cells derived from HLA-C1 donor (F) and derived from HLA-C2 donor (G).

(I) Comparison of frequencies of effector memory $CD8^+$ T cells in EBV infected single and mixed reconstituted huNSG mice at experimental endpoints in spleen.

Data are pooled data from at least two independent experiments. n=5-8 mice per group, mean ± SEM, unpaired t test, n.s., not significant.

Figure S6
related to Figure 7

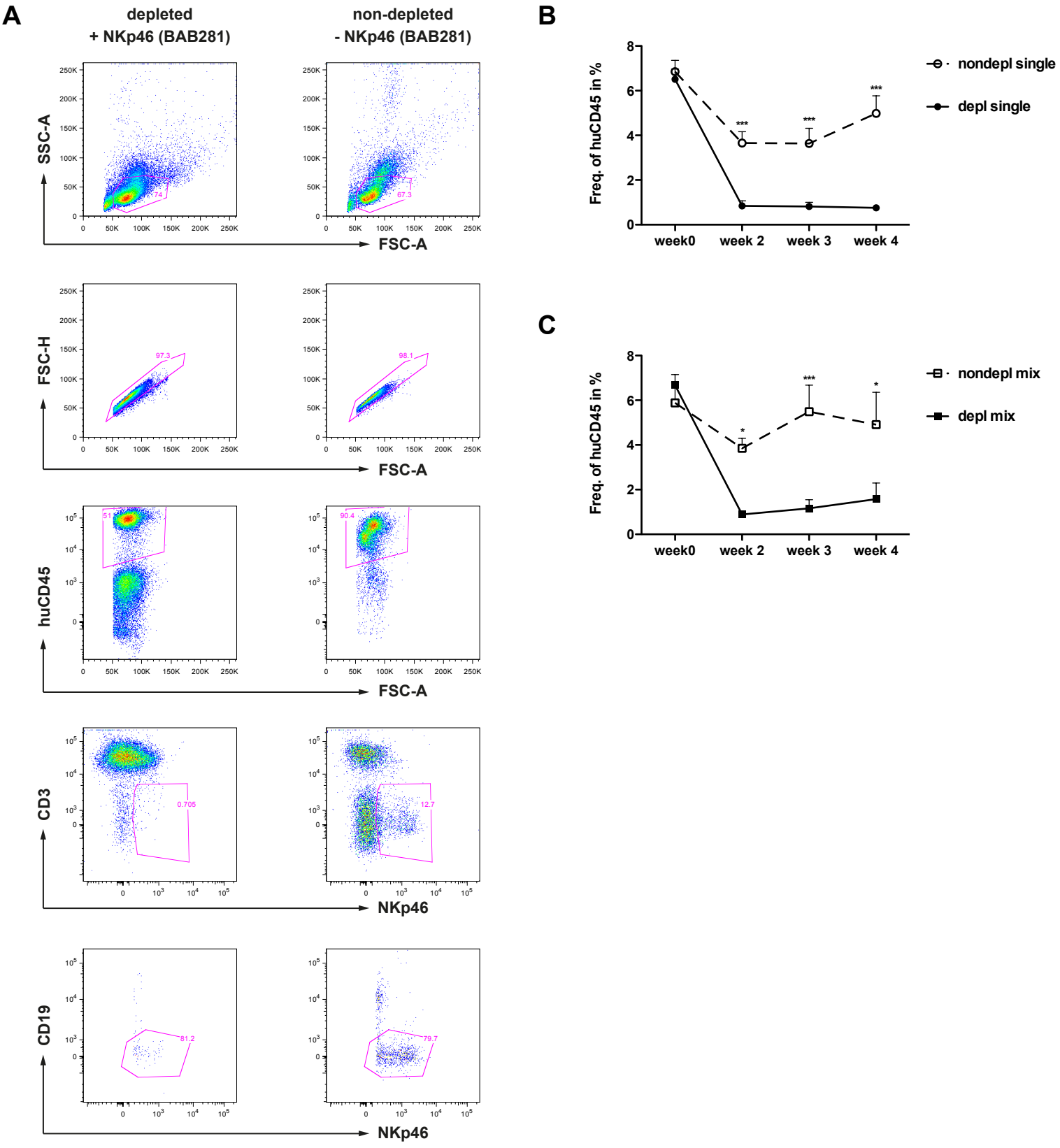

Figure S6, related to Figure 7. NKp46 mediated depletion of NK cells persists throughout the duration of the experiment.

NK cells in huNSG mice were depleted by i.p. injection of NKp46 binding antibody (clone BAB281) on 3 consecutive days prior to infection with EBV. Depletion of NK cells over the course of the experiment was assessed by flow cytometry. (A) Cells were pre-gated on lymphocytes and singlets before discriminating for the huCD45$^{\pm}$ population. NK cells were defined as huCD45$^{\pm}$ CD3^{-} NKp46$^{\pm}$ CD19^{-} events. In both single (B) and mixed reconstituted huNSG mice (C) NK cell frequencies of depleted animals remained low throughout the duration of the experiment.

Figure S7

related to Figure 7

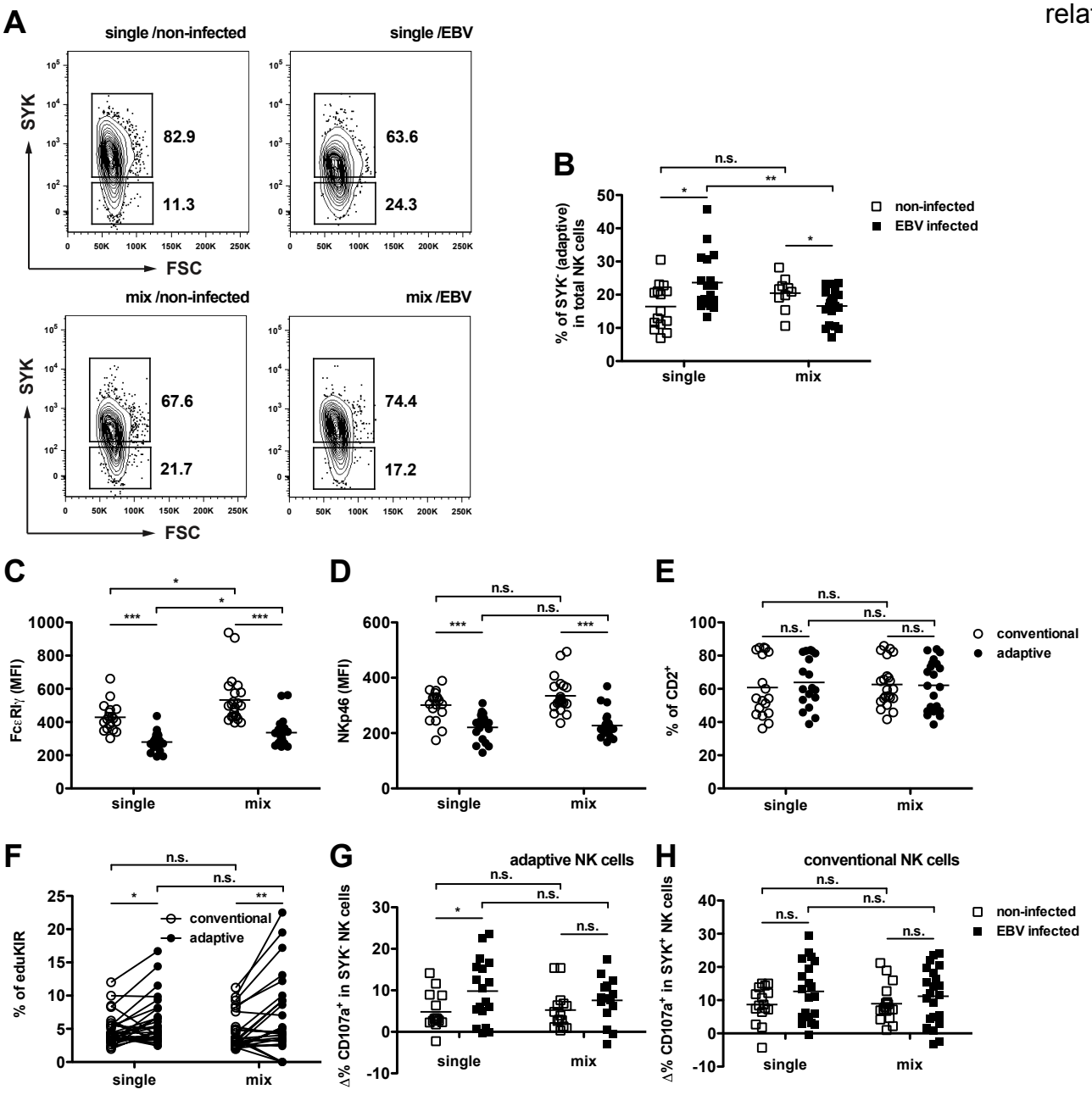

Figure S7, related to Figure 7. No expansion of NK cells with an adaptive phenotype in mixed reconstituted huNSG mice.

(A) Representative dot plots showing expression of SYK in splenic NK cells from single and mixed reconstituted huNSG mice infected or not with EBV.

(B) Frequency of SYK$^-$ (adaptive) splenic NK cells in single and mixed reconstituted huNSG mice 5 weeks after EBV infection compared to non-infected controls (n=10-21 mice per group).

(C to F) SYK$^\pm$ (conventional) and SYK$^-$ (adaptive) splenic NK cells in single and mixed reconstituted huNSG mice 5 weeks after EBV infection compared for expression (median fluorescence intensity, MFI) of FcεRIγ (C), NKp46 (D), frequency of CD2 expression (E) and frequency of educated (eduKIR) NK cells (F). n=18-28 mice per group.

(G and H) Degranulation of splenic NK cells with adaptive (SYK$^-$) phenotype (G) and conventional (SYK$^\pm$) phenotype (H) in single and mixed reconstituted huNSG mice 5 weeks after EBV infection compared to non-infected controls after CD16 stimulation. Δ%CD107a refers to the difference of degranulation with and without CD16 stimulation. Average ± s.e.m. of spontaneous degranulation was 5.85 % ± 0.66. (n=15-22 mice per group).

Data are pooled data from at least two independent experiments. Bar represents mean. Data were analyzed by multiple t tests, *p < 0.05, p** < 0.01, p*** < 0.001.

Supplemental Experimental Procedures

Table S1. Overview of fluorescently labeled antibodies

Molecule	Clone	Fluorophore	Company
CD107a	H4A3	FITC	BD Biosciences
NKp46	9E2	APC	BD Biosciences
KIR2DL1/S1	EB6B	PE Cy7	Beckman&Coulter
KIR2DL2/L3	GL183	PE Cy5.5	Beckman&Coulter
NKG2A	Z199	PE	Beckman&Coulter
CD14	M5E2	BV510	BioLegend
CD16	3G8	APC Cy7	BioLegend
CD19	HIB19	BV510	BioLegend
CD2	RPA-2.10	FITC	BioLegend
CD3	OKT3	BV510	BioLegend
CD3	OKT3	BV785	BioLegend
CD4	RPA-T4	APC Cy7	BioLegend
CD4	RPA-T4	BV510	BioLegend
CD45	HI30	BV605	BioLegend
CD45RA	HI100	BV510	BioLegend
CD57	HCD57	Pacific Blue	BioLegend
CD8	SK1	PerCP	BioLegend
HLA-A2	BB7.2	APC Cy7	BioLegend
HLA-A2	BB7.2	FITC	BioLegend
HLA-A2	BB7.2	Pacific Blue	BioLegend
HLA-A2	BB7.2	PE	BioLegend
HLA-DR	L243	PE Cy7	BioLegend
KIR2DL1/S1	HP-MA4	FITC	BioLegend
KIR2DL2/L3	DX27	PE	BioLegend
KIR2DL2/L3	DX27	PE Cy7	BioLegend
KIR3DL1	DX9	Alexa Fluor 700	BioLegend
KIR3DL1	DX9	PE Cy7	BioLegend
Syk	4D10.2	PE	BioLegend
CD19	SJ25-C1	PE Texas Red	invitrogen
FcεRIγ	Polyclonal	FITC	Merck Millipore
CCR7	150503	PE	R&D Systems